RESEARCH PAPER

PCCP
www.rsc.org/pccp

Theoretical and experimental evaluation of the radial function for electric dipole moment of hydrogen iodide

Joost N. P. van Stralen,[a] Lucas Visscher*[a] and J. F. Ogilvie[b]

[a] *Department of Theoretical Chemistry, Faculty of Sciences, Vrije Universiteit Amsterdam, De Boelelaan 1083, Amsterdam 1081 HV, The Netherlands. E-mail: visscher@chem.vu.nl*
[b] *Escuela de Quimica, Universidad de Costa Rica, San Pedro de Montes de Oca, San Jose 2060, Costa Rica*

Received 13th February 2004, Accepted 21st May 2004
First published as an Advance Article on the web 27th May 2004

From relativistic quantum-chemical calculations of the molecular electronic structure of hydrogen iodide HI in electronic state X $^1\Sigma^+$ or 0^+ using the Dirac–Coulomb coupled-cluster method with singles, doubles and non-iterative triples (DC-CCSD(T)), we have evaluated the electric dipole moment p at 17 values of internuclear distance R. On this basis we have calculated the pure vibrational expectation value in the vibrational ground state and matrix elements of $p(R)$ for transitions from that ground state to the first seven vibrationally excited states within the electronic ground state. For comparison with these theoretical results, we have undertaken a re-analysis of all experimental data of intensities of vibration-rotational transitions in infrared spectra, combined with a value of the expectation value of $p(R)$ in the ground state from the Stark effect, to generate a radial function for electric dipole moment. The agreement between calculated and experimental values of vibrational matrix elements of the electric dipole moment is satisfactory, resolving outstanding questions about experimental and computational accuracy in the literature. We predict matrix elements for intensities of vibration-rotational bands 6–0 and 7–0, not yet measured.

I Introduction

The objective of our present work is to re-examine the theoretical dipole moment of HI using state-of-the-art quantum-chemical methods, expecting that there is room for improvement of the theoretical results reported by Ilias *et al.*[1] In particular, we investigate whether their suspicion of experimental data is well founded. For the purpose of such an examination, it is essential that also all secondary experimental data be subjected to critical analysis. We therefore also generated a new potential–energy curve and a new radial function for electric dipole moment directly from experimental data according to well developed methods.[2]

Many researchers have undertaken calculations on the electric dipole moment of the hydrogen iodide molecule, either only at the equilibrium internuclear distance R_e or as a function of distance R.[1,3–14] After non-relativistic calculations at the end of the 1970s and beginning of the 1980s,[3,4] the first relativistic calculations appeared in the middle of the 1980s;[5–7] in the 1990s the latter calculations, combined with sophisticated methods to describe electron correlation, yielded results in reasonable agreement with experiment.[8–10] Of previous publications on the dipole moment of HI, only some recent, and—for our purpose—relevant ones are summarised below.

Alekseyev *et al.*[12] employed a scalar relativistic effective core potential (RECP) in their multi-reference configuration-interaction (MR-CI) calculation of the dipole-moment function of HI. After inclusion of a spin–orbit coupling (SOC) contribution –0.009 au, their result, 0.176 au, coincided with the experimental value for the dipole moment at R_e.[15] This agreement should, however, be considered fortuitous because their basis set contained only one f function and no higher angular-momentum functions, and was hence too small to prevent significant basis-set truncation errors. The RECP treatment of relativistic effects on the dipole moment was proven to be reliable by Norman *et al.*[13] who performed non-relativistic (NR), RECP, Douglas–Kroll–Hess (DKH) and Dirac–Coulomb (DC) Hartree–Fock (HF) calculations of static response properties, at R_e, of hydrogen halides.

Maroulis[11] performed NR-CCSD(T) calculations with a larger basis and supplemented these with a relativistic correction −0.040 au taken from the work of Kellö and Sadlej.[8] On the basis of a 9% discrepancy between his computed $p(R_e) = 0.191$ au and the experimental value, Maroulis suggested that new measurements of dipole moment be performed. Ilias *et al.*[1] reported an extensive study of correlation and relativistic effects on the dipole moment and dipole polarizability; they included relativistic effects by means of the DKH Hamiltonian using also the CCSD(T) method to account for electron correlation. Through estimation of the omitted small effect of SOC by configuration–interaction calculations, they reported a value 0.154 ± 0.03 au that deviated significantly from Maroulis's value and from the experimental value; they also concluded that the experimental values of the dipole moment and its first derivative with the distance were inaccurate.

The dependence of the dipole moment on the internuclear distance is not observed directly but derived from infrared absorption spectra. Experimental measurements of spectral intensities of lines in the infrared bands of a diatomic species in absorption yield data from which a radial function for the electric dipole moment is deduced. Although there is no measurement of intensity in the pure rotational band of HI, a measurement by van Dijk and Dymanus[15] of the Stark effect on the first transition in that band yielded an expectation value $\langle 0|p(R)|0\rangle = 0.4477 \pm 0.0005$ D $= 0.1761 \pm 0.0002$ au that underlies the value of p at R_e questioned by Maroulis and by Ilias *et al.* Ameer and Benesch,[16] Niay *et al.*[17], Riris *et al.*[18] and Bulanin *et al.*[19] measured the intensities of lines of HI in the fundamental vibration–rotational band with increasing precision in that chronological order. Benesch[20], Meyer *et al.*[21] and Bulanin *et al.*[22] measured the intensities of lines of HI in band $v' = 2 \leftarrow v = 0$. Meyer *et al.*[21] and Riris *et al.*[18] published measurements of intensities in band $v' = 3 \leftarrow v = 0$, and Niay *et al.*[23] reported that their own measurements verified those of

DOI: 10.1039/b402158d

Meyer *et al.*[21] as presented in Haeusler's thesis.[24] For bands $v' = 4,5 \leftarrow v = 0$, Niay *et al.*[23] reported the only known data. Besides these reports of measured intensities, there are many measurements of frequencies for both HI and DI, from the pure rotational bands to the sixth overtone $v' = 7 \leftarrow v = 0$.

II Methods and computational details for electronic structure

The most important factors determining the quality of theoretical calculations on molecules containing only light elements are the treatment of electron correlation and the basis set.[25] For molecules containing heavy elements, such as iodine in this case, relativistic effects become also important.[26] In the following paragraphs we describe how we treat these aspects in our calculations.

For hydrogen, we used the same basis set as for the calculation of the electric field gradient in HI,[27,28] which is the Sadlej basis[29] extended with additional tight p and d functions. For iodine, we generated a new basis: we applied a strategy similar to that in previous work on electric field gradients,[27,28,30] according to which we extend the basis set until the value of the property studied converges within a certain criterion. Specifically for iodine, we began with the same optimised atomic Dirac–Coulomb Hartree–Fock (DC-HF) basis as in our previous calculations for iodine compounds,[28] which is a 26*s*19*p*13*d* even-tempered dual-family basis set augmented with two f functions. Beginning at $l = 0$ we added individual functions on the small exponent side of the range until the DC-HF dipole moment of HI altered less than 0.001 au. At that point, we began to add functions on the large exponent side. This process of successively adding diffuse-like and tight-like functions was repeated for values of l up to four. For correlated calculations the requirements of a basis set are more severe than for uncorrelated calculations.[31] To ensure that our basis set is adequate for describing the dipole moment of HI at the correlated level, we tested the convergence of the dipole moment also at the spin-free Dirac–Coulomb (SFDC) CCSD level. We specifically investigated the convergence of the dipole moment by adding complete diffuse *spdfgh* shells to the iodine basis. The results of this study on the influence of the basis set on the computed dipole moment are reported in the Results section.

To describe the effect of electron correlation, we applied the CCSD(T) method. For reasons of computational efficiency, we used spinors in the energy range only between -15 E_h and $+50$ E_h in the correlated calculations. Contributions from core spinors and from virtual spinors with higher energies are negligible (less than 0.0002 au), as was verified in several test calculations at the DC-MP2 and SFDC CCSD levels of theory, respectively.

The DC Hamiltonian includes all relativistic effects, which makes direct comparison with earlier calculations difficult. To assess the relative importance of scalar and SOC effects, we therefore also performed non-relativistic calculations using the Lévy–Leblond Hamiltonian[32] and scalar relativistic calculations using the SFDC formalism of Dyall.[33]

In all calculations of the electronic structure we used the DIRAC program[34] and conformed to our customary procedure of neglecting the numerous two-electron integrals that involve only the small component, S, of the wave function.[35] Test calculations show that this omission gives an error less than 0.00001 au, in this case. To calculate the dipole moments we added the HF expectation value and the finite-field correlation contributions computed using field strengths +0.0005 and −0.0005 au. We calculated 17 dipole moments in the range $R/10^{-10}$ m = [1.2, 1.9] and fitted these to a polynomial in the reduced coordinate $x = (R-R_e)/R_e$.

Although the basis set was optimised for our main interest—the dipole moment—we expect this basis to be also adequate for spectral parameters. We obtained spectral parameters with the CCSD(T) method, with the same active space as for calculations of the dipole moment. Two-electron integrals of the type (SS|SS) were again neglected. We calculated 19 energy points in the range $R/10^{-10}$ m = [0.8, 2.5] and corrected all these points for basis-set superposition errors. The minimum of each curve was obtained with a cubic fit, using five points about the minimum, spaced 1 pm from each other. Other spectral parameters were obtained on fitting energies of vibration–rotational states $E(v,J)$, obtained through use of the LEVEL program,[36] to the expression

$$E(v,J) = -D_e + \omega_e\left(v+\tfrac{1}{2}\right) - \omega_e x_e\left(v+\tfrac{1}{2}\right)^2 + \omega_e y_e\left(v+\tfrac{1}{2}\right)^3 + B_v J(J+1) \quad (1)$$

with

$$B_v = B_e - \alpha_e\left(v+\tfrac{1}{2}\right). \quad (2)$$

III Results

Dipole-moment functions from quantum-chemical calculations

In this section, we compare the effects of basis set, electron correlation and relativity on the dipole-moment function. To allow a fair study of the effect of one parameter on the dipole-moment function, we tried to eliminate errors in other parameters as much as possible to avoid interference and cancellation of errors. For example, when seeking the effect of relativity on the dipole moment, we used the CCSD(T) method to describe electron correlation and applied our best basis set.

Table 1 presents the results of our study of the basis set: the upper part shows the variation of the dipole moment at the DC-HF level on extending the basis set, as described in the preceding section; the lower part shows the analogous variation at the SFDC-CCSD level (at the HF level only the additions of the basis functions that contribute sufficiently to be retained in the set are shown). At the DC-HF level, few basis functions are required to make the dipole moment converge. Evident are the additions of a diffuse p function, which has exponent 0.0441, that contributes −0.0257 au, and of two diffuse d functions, which have exponents 0.2255 and 0.1007,

Table 1 Convergence of the dipole moment p at R_e on the systematic extension of the basis set; the upper part corresponds to Dirac–Coulomb Hartree–Fock values, the lower part to spin-free CCSD values. For the Hartree–Fock values only the relevant values are shown

Basis I		p/au	Δp/au
	DC-HF		
[26*s*19*p*13*d*]	(b1):	−0.1699	
[26*s*19*p*13*d*2*f*]	(b2): (b1 + 2 diffuse *f*)	−0.1664	0.0035
[26*s*20*p*13*d*2*f*]	(b3): (b2 + diffuse *p*)	−0.1921	−0.0257
[26*s*20*p*14*d*2*f*]	(b4): (b3 + diffuse *d*)	−0.1955	−0.0086
[26*s*20*p*15*d*2*f*]	(b5): (b4 + diffuse *d*)	−0.2000	−0.0115
[26*s*20*p*15*d*2*f*1*g*]	(b6): (b5 + tight *g*)	−0.1988	0.0012
	SFDC-CCSD		
[26*s*20*p*15*d*2*f*1*g*]	(b7): (b6)	−0.1648	
[26*s*20*p*15*d*3*f*1*g*]	(b8): (b7 + tight *f*)	−0.1633	0.0015
[26*s*20*p*15*d*4*f*1*g*]	(b9): (b8 + tight *f*)	−0.1627	0.0006
[27*s*21*p*16*d*4*f*2*g*1*h*]	(b10): (b8 + diffuse *spdfgh*)	−0.1853	−0.0220
[28*s*22*p*17*d*5*f*3*g*2*h*]	(b11): (b10 + diffuse *spdfgh*)	−0.1880	−0.0027
[29*s*23*p*18*d*6*f*4*g*3*h*]	(b12): (b11 + diffuse *spdfgh*)	−0.1880	0.0000
[28*s*22*p*17*d*5*f*3*g*2*h*1*i*]	(b13): (b11 + diffuse *i*)	−0.1879	0.0001
[29*s*23*p*18*d*6*f*4*g*3*h*]	(b14): (b11 + tight *spdfgh*)	−0.1880	−0.0001

[a] Sadlej's basis set29 plus extra tight p and d functions27 resulting in a 11*s*6*p*3*d* set; this basis is large enough to fulfil the desired criteria.

with contributions −0.0086 au and −0.0115 au, respectively. Addition of the first diffuse shell for the correlated calculations is important: the SFDC-CCSD value is altered by 0.0221 au. An addition of an *i* function and of a tight shell of *spdfgh* functions is unimportant. The final basis set for which the SFDC-CCSD dipole moment alters less than 0.001 au with respect to the next basis is a 28*s*22*p*17*d*5*f*3*g*2*h* basis. By applying this basis set in the correlated DC calculations, we obtained an accurate theoretical dipole-moment function of HI.

Fig. 1 shows the dipole moments as a function of R for some basis sets listed in Table 1. Both the magnitude of the dipole moment near R_e and the dependence of the dipole moment on the distance alter significantly on proceeding from small to large basis sets, underlining the importance of employing large basis sets in the calculation.

In Fig. 2 we present curves for $p(R)$ for electron-correlation methods MP2, CCSD and CCSD(T). We performed these calculations using the DC Hamiltonian and a 28*s*22*p*17*d*5*f*3*g*2*h* basis. This plot demonstrates that the perturbative MP2 approach fails even for small displacements from R_e, as noted by Maroulis.[11]

Fig. 3 shows curves for $p(R)$ calculated using various Hamiltonians; the NR results are calculated using the Lévy–Leblond Hamiltonian and the SFDC results using the spin-free Hamiltonian of Dyall, whereas the DC results are the full Dirac–Coulomb results, all at the CCSD(T) level. The new experimental curve is explained in the subsection on analysis of spectral data and in the discussion.

A fit of the DC-CCSD(T) points of calculated dipole moment to a polynomial in x for comparison with previous results yielded this formula,

$$\begin{aligned} p(x)/\text{au} = {} & (0.1735667 \pm 0.0000053) \\ & - (0.03712 \pm 0.00008)x + (0.2258 \pm 0.0005)x^2 \\ & - (0.8068 \pm 0.0053)x^3 - (0.0440 \pm 0.0132)x^4 \\ & + (0.369 \pm 0.103)x^5 + (0.863 \pm 0.116)x^6 \\ & + (0.124 \pm 0.743)x^7 - (11.18 \pm 0.46)x^8 \\ & + (16.76 \pm 2.15)x^9 + (11.9 \pm 0.7)x^{10} \\ & - (24.0 \pm 2.1)x^{11} \end{aligned} \qquad (3)$$

in which the uncertainties specified as single standard deviations represent only the error of fitting to that polynomial. An essentially exact fit of the 17 computed points, within the last digit of each computed value, required a polynomial of degree 11. The terms beyond x^7 have little statistical or physical significance and reflect merely the constraint to an exact fit; these terms are not further used.

An analogous fit of computed energies to provide a potential-energy curve was impracticable because the computed points are not spaced sufficiently densely for this purpose. As the study of the dipole-moment function was our main interest, we therefore chose to combine the computed dipole-moment function with a function for potential energy derived from experimental data. With the above theoretical function for electric dipole moment, this function, according to the coefficients presented in Table 2, produced theoretical estimates of matrix elements of electric dipole moment for vibrational transitions presented in Table 3.

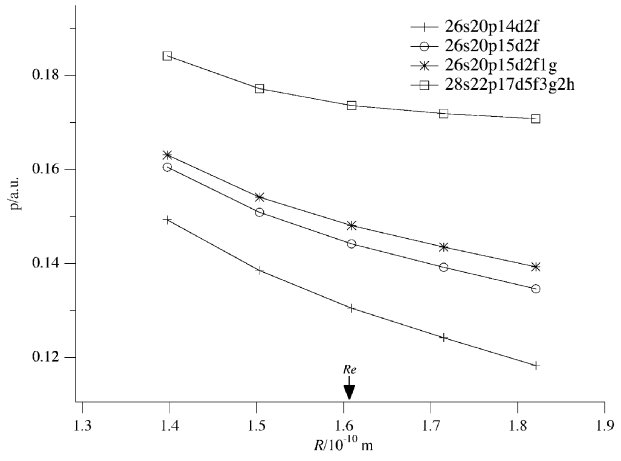

Fig. 1 DC-CCSD(T) dipole moment *p versus* internuclear distance in a region $R/10^{-10}$ m = [1.4, 1.8] using various basis sets for iodine. The position of R_e is indicated with an arrow.

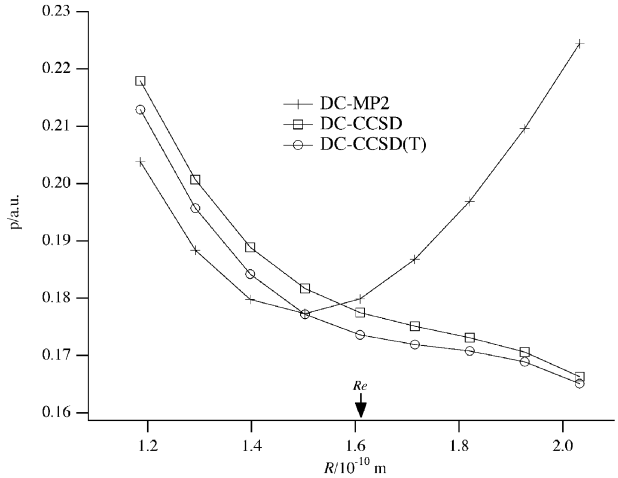

Fig. 2 Dipole moment *p versus* internuclear distance in the region $R/10^{-10}$ m = [1.2, 2.0] using various correlated methods. The position of R_e is indicated with an arrow.

Spectral parameters from quantum-chemical computations

For transitions involving only the lower vibrational states it is possible to calculate spectral parameters with reasonable accuracy. We have done so at the CCSD(T) level of theory using the Lévy–Leblond, spin-free and Dirac–Coulomb Hamiltonians, and also using the SFDC-CCSD(T) energies augmented with HF SOC contributions; the results for these parameters are collected in Table 4. The experimental equilibrium binding energy, D_e, combines a value of the spectral dissociation energy D_0 from the literature[37] with a zero-point vibrational energy from our analysis of frequency data.

Analysis of spectral data

A detailed overview of methods to fit experimental data to a potential-energy curve in various functional forms appears

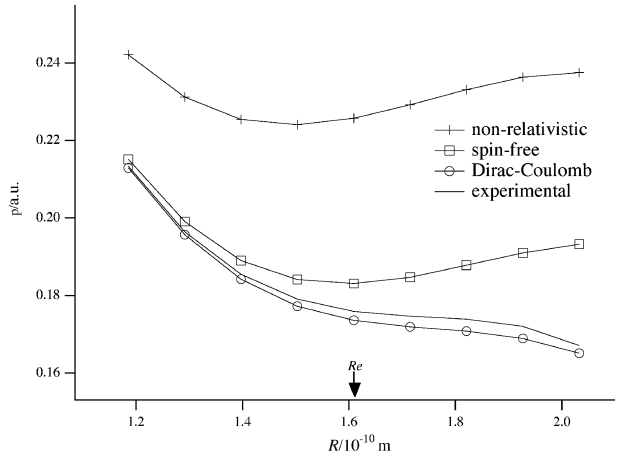

Fig. 3 Dipole moment *p versus* internuclear distance in the region $R/10^{-10}$ m = [1.2, 2.0] calculated with various Hamiltonians; experimental values correspond to the new dipole-moment function (eqn. (7)). The position of R_e is indicated with an arrow.

Table 2 Values of parameters fitted or constrained in analysis of frequency data of HI and DI

Parameter	Value	Uncertainty
c_0/m^{-1}	20469900	81
c_1	−1.547358	0.000197
c_2	0.985396	0.00075
c_3	−0.5809	0.0135
c_4	−0.0369	0.074
c_5	−0.446	0.26
c_6	3.08	2.5
c_7	−0.12	6.0
c_8	−42.6	17.
${s_0}^H$	0.6659	0.0025
${t_0}^H$	[0.1908]	
${t_1}^H$	0.0540	0.0164
${t_2}^H$	[0]	
${t_3}^H$	−13.11	1.44
${t_0}^I$	[0.0749]	
${u_1}^H/10^6\ \mathrm{m}^{-1}$	−4.4082	0.0161
${u_2}^H$	[0]	
${u_3}^H/10^6\ \mathrm{m}^{-1}$	10.96	0.78
${u_4}^H/10^6\ \mathrm{m}^{-1}$	41.9	3.7
$R_e/10^{-10}$ m	1.60904898	0.00000055

[a] Values enclosed within brackets are constrained; the uncertainty of R_e includes error of fundamental constants h and N_A. The maximum range of validity of pertinent radial functions is $R/10^{-10}\ \mathrm{m} = [1.3, 2.3]$.

elsewhere.[2] We fitted frequencies and wave numbers of pure rotational and vibration-rotational transitions from the available experimental data, summarised in Table 5, to Dunham coefficients Y_{kl}. With a minimal number of coefficients, consistent with constraints through parameters c_j, a potential-energy curve,

$$V(z) = c_0 z^2 \left(1 + \sum_{j=1} c_j z^j\right) \tag{4}$$

was defined that is practically independent of nuclear mass. In eqn. (4), $z = 2(R - R_e)/(R + R_e)$ is a reduced displacement variable. Other coefficients, s_j, t_j and u_j, explained below, are related to vibrational and rotational g factors and adiabatic corrections, respectively, for each atomic type, and were included empirically within applicable auxiliary coefficients Z_{kl} (ref. 2) to yield the best fit of the available experimental data of frequency type. All coefficients Y_{kl} and Z_{kl} beyond the minimal range defined consistently through these radial coefficients are taken to have zero value, but further radial coefficients of types c_j, s_j, t_j and u_j in several series are merely indeterminate and have not a zero value in general. Like c_9 and c_{10}, not listed in Table 2 as they pertain to bands for which no experimental intensity data are reported, values of other radial coefficients are irrelevant for the present work.

To take into account extra-mechanical effects due to electrons imperfectly following rotational and vibrational motions of the nuclei, we include parameters u_1, u_3 and u_4 for adiabatic effects, s_0 related to the vibrational g factor at R_e and t_1 and t_3 related to the radial function for the rotational g factor.[2] Parameters u_2 and t_2 that occur in only linear manner were constrained to zero during the fit because, when left freely adjustable, their values were zero within their estimated standard errors. We constrained values of ${t_0}^H$ and ${t_0}^I$ to values consistent with the measured rotational g factor, $g_r(R_e) = 0.096 \pm 0.010$ [38] and permanent electric dipole moment,[15] as described elsewhere.[39] The values of all these parameters are

Table 3 Pure vibrational matrix elements of electric dipole moment from theoretical calculations and from fits of intensities of individual lines in vibration-rotational bands of HI, Herman–Wallis coefficients $C_0^{v'}$ and $D_0^{v'}$, and sources of intensity data

Band	$\langle v'\|p(R)\|0\rangle$/C m	$C_0^{v'}$	$D_0^{v'}$	Ref.
0–0	1.4731×10^{-30}[a]			
	$(1.4934 \pm 0.0017) \times 10^{-30}$[b]			
1–0	-1.6672×10^{-32}[a]	0.1323[c]	0.0035[c]	
	$(-1.358 \pm 0.011) \times 10^{-32}$[d]	0.13191 ± 0.00001[d]	0.00442 ± 0.00001[d]	19
2–0	7.1788×10^{-33}[a]	0.0317[c]	0.00025[c]	
	$(6.582 \pm 0.033) \times 10^{-33}$[d]	0.03099 ± 0.00001[d]	-0.000244 ± 0.000001[d]	22
3–0	-4.0211×10^{-33}[a]	0.0116[c]	0.000023[c]	
	$(-4.085 \pm 0.42) \times 10^{-33}$[d]	0.0088 ± 0.0015[d]	-0.00156 ± 0.00014[d]	18,21
4–0	1.4325×10^{-33}[a]	0.0163[c]	0.000066[c]	
	$(1.332 \pm 0.156) \times 10^{-33}$[d]	0.0213 ± 0.0008[d]	0.0020 ± 0.0001[d]	23
5–0	-4.7745×10^{-34}[a]	0.0169[c]	0.00024[c]	
	$(-4.521 \pm 0.052) \times 10^{-34}$[d]	0.0143 ± 0.0013[d]	0.0027 ± 0.0002[d]	23
6–0	1.6896×10^{-34}[a]			
7–0	-6.2495×10^{-35}[a]			

[a] From theoretical calculations. [b] From the Stark effect, reference 15. [c] Calculated with $p(x)$ from experiment. [d] From direct fitting of experimental data in the specified references.

Table 4 Spectral parameters from CCSD(T) calculations compared with those from experiment; NR signifies non-relativistic, SFDC spin-free, SOC spin–orbit coupling and DC Dirac–Coulomb

	NR	SFDC	SFDC + SOC correction[a]	DC	Feller *et al.*[b]	Experiment
$R_e/10^{-10}$ m	1.6178	1.6107	1.6136	1.6136	1.5998	$1.60904898 \pm 0.00000055$
$\omega_e/\mathrm{cm}^{-1}$	2338.65	2320.11	2298.64	2298.71	2354.70	2309.095845 ± 0.000053
$x_e\omega_e/\mathrm{cm}^{-1}$	38.15	38.09	38.81	38.85		39.6077 ± 0.0064
D_e/kJ mol^{-1}	335.7	331.0	302.5	303.7	311.7	308.3 ± 0.2[c]
B_e/cm^{-1}	6.441	6.497	6.475	6.476		$6.511907129 \pm 0.000000042$
$\alpha_e/\mathrm{cm}^{-1}$	0.164	0.167	0.171	0.172		0.170450 ± 0.000022

[a] Based on a potential-energy curve from SFDC-CCSD(T) energies plus HF SOC contributions. [b] Ref. 44. [c] Ref. 37 plus zero-point energy 13.692430 kJ mol^{-1}.

Table 5 Sources of data for derivation of a function for potential energy of HI

Band	Number of lines	Ref.	Number of lines	Ref.	Number of lines	Ref.
	HI		DI		TI	
0–0	2	46	3	46	1	47
0–0	11	48	9	49		
1–0	24	50	28	51		
2–0	34	51	40	51		
3–0	34	51	39	51		
3–0			6	52		
4–0	31	51	34	51		
4–0			4	52		
5–0	24	51	29	51		
5–0	1	23	3	52		
6–0	30	53				
7–0	18	53				

listed, with their uncertainties as single standard errors, in Table 2. With these values of radial parameters, we then calculated the values of the experimental spectral parameters reported in the latter column of Table 4, except D_e that is indeterminate from infrared data.

After deriving this potential–energy curve, we collected all known data[16–24] of intensities of spectral lines in vibration-rotational bands of $^1H^{127}I$ into a spreadsheet, converted them to squares of individual vibration-rotational matrix elements $|\langle v', J'|p(R)|0, J''\rangle|^2$, and scrutinised these values taking into account their individual or collective uncertainties of measurement. We transferred the data for each band to a Maple worksheet and applied a method—weighted linear regression with criterion of least sum of weighted squares of residuals—to estimate from individual measurements of squares of vibration-rotational matrix elements the square of the pure vibrational matrix element $|\langle v'|p(R)|0\rangle|^2$ and Herman–Wallis coefficients $C_0^{v'}$ and $D_0^{v'}$ for each band according to the relation[2]

$$|\langle v', J'|p(R)|0, J''\rangle|^2 = |\langle v'|p(R)|0\rangle|^2\left(1 + C_0^{v'}\iota + D_0^{v'}\iota^2\right) \quad (5)$$

in which running number ι is defined to be $\iota = 1/2[J'(J'+1) - J''(J''+1)]$. The source of particular data for each band used is identified in Table 3 with results of these fits; for band $v' = 3 \leftarrow v = 0$, we combined old data[21] with more recent data[18] by scaling the former to be consistent with the latter, because the latter data are sparse.

Assuming a radial function of the form $p(x) = \sum_{j=0} p_j x^j$, to conform to previous notation,[40] we solved a system of linear simultaneous equations

$$\langle v'|p(x)|0\rangle = \sum_j p_j x^j \langle v'|x^j|0\rangle, j = 0..5 \quad (6)$$

in which pure vibrational matrix elements $\langle v'|x^j|0\rangle$ are calculated directly from symbolic expressions[2,41] involving coefficients c_j of potential energy presented in Table 2. The resulting radial function for electric dipole moment is

$$p(x)/\text{au} = 0.1759 - 0.030x + 0.2234x^2 - 0.7925x^3 - 0.2363x^4 - 0.6243x^5 \quad (7)$$

Fig. 4 presents a curve of this function in R in a range $R/10^{-10}$ m = [1.25, 2.25], with a graphical representation of the theoretically derived function (eqn. (3)).

We evaluated the signs of $\langle v'|p(R)|0\rangle$, indicated with superscript suffix c in Table 3, to produce best agreement between calculated values of Herman–Wallis coefficient $C_0^{v'}$, indicated with suffix d in Table 3, and the corresponding experimental values. Calculated values of both $C_0^{v'}$ and $D_0^{v'}$ are based on trial $p(x)$ through algebraic expressions.[2,41]

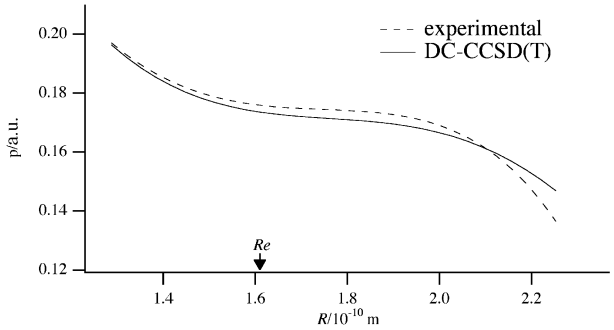

Fig. 4 Theoretical and experimental radial functions $p(R)$ of the electric dipole moment from eqns. (3) and (7).

IV Discussion

Dipole-moment function

The experimental radial function for electric dipole moment (eqn. (7)) agrees satisfactorily with the theoretical one (eqn. (3)). This condition is reflected in the agreement between the theoretical values of matrix elements of $p(R)$ for vibrational transitions and the experimental values up to $v' = 5$, both shown in the second column of Table 3. Most errors are within a few per cent with the largest deviation for $\langle 1|p(R)|0\rangle$, that is about 25 per cent too large. That the slope of $p(R)$ near R_e is atypically small leads to a large relative error; the absolute error is modest in all computed matrix elements. On this basis, we have confidence that predictions for $\langle 6|p(R)|0\rangle$ and $\langle 7|p(R)|0\rangle$ in the above table will also prove accurate within 10 per cent.

Use of a method better than CCSD(T) to achieve higher-order correlation might further improve agreement with experimental results. Fortuitous cancellation of errors in the CCSD method likely produces agreement with experiment slightly better than with CCSD(T) for the dipole moment at R_e. For other coefficients of the dipole moment the CCSD(T) results agree better with experiment. For distances with $R/10^{-10}$ m > 2.5, the CCSD method appears superior. In Fig. 5 we plot the dipole moment for CCSD, CCSD(T) and the Padé function from 1980[40] in a range $R/10^{-10}$ m = [0.24, 4.8]. The Padé function is a combination of experimental data near R_e with the non-relativistic two-configuration MCSCF calculations of Ungemach *et al.*[3] for R at long range. The CCSD plot follows the Padé function, with its correct asymptotic behaviour, over a greater range of R better than the CCSD(T) curve. This result is likely comparable to the superior behaviour of CCSD compared to CCSD(T) for the potential-energy curve of molecules HF and F_2.[42] The reason is that the (T) correction is based on a fifth-order perturbation expression that diverges for nearly degenerate wave functions. CCSD itself, as an iterative or infinite-order method, is not based on the perturbation theory and thus provides a better description

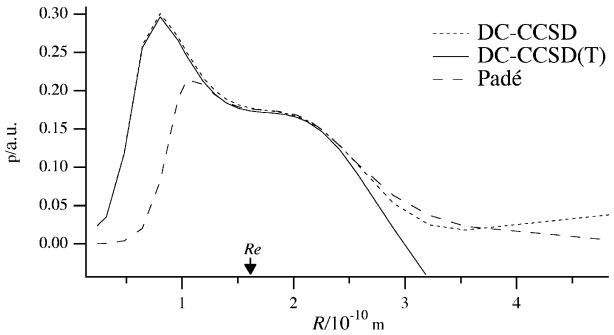

Fig. 5 Comparison of the DC-CCSD, DC-CCSD(T) and Padé[40] dipole moment $p(R)$ over a large range of distance.

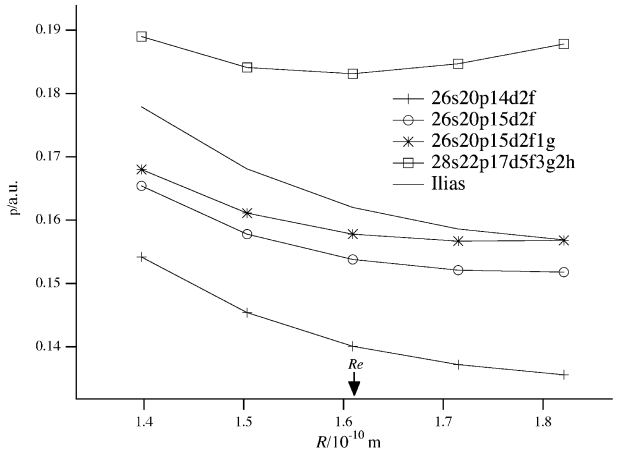

Fig. 6 SFDC-CCSD(T) dipole moment *p versus* internuclear distance in the region $R/10^{-10}$ m = [1.4, 1.8] using various basis sets for iodine; the 'Ilias' curve is obtained from ref. 1. The position of R_e is indicated with an arrow.

at large R. For $R/10^{-10}$ m < 1.1 the coupled-cluster and Padé functions begin to deviate from each other. The coupled cluster values in this region are probably nearer the true values than the Padé function because the latter, for small R, is based on a functional form that is correct only in a limiting region $R = 0$.

Comparison of the plots based on various Hamiltonians with the curve from experiment (Fig. 3) makes clear that relativistic effects are important to render an accurate description of the dipole-moment function of HI. The slope of the scalar relativistic dipole-moment function has the wrong sign at distances larger than R_e; apparently SOC is important not only for a quantitative description of the dipole moment of HI near R_e but also for a qualitative description of its dependence on the internuclear distance. This effect might be due to an avoided crossing allowed through SOC, but analysis of this point is difficult in our calculations. The importance of this spin–orbit interaction furthermore indicates that even inclusion of the two-electron Gaunt interaction in the Hamiltonian might be required to improve on the DC-CCSD(T) results.

The curves for non-relativistic and scalar relativistic CCSD(T) dipole moments of Maroulis[11] and of Ilias *et al.*[1] show no increase in the dipole moment on increasing internuclear distance near R_e. To rationalize this difference with our DC-CCSD(T) results, we plot the SFDC-CCSD(T) curve for the dipole moment of HI in Fig. 6. Improving the quality of the basis set not only raises the curve for the dipole moment but also greatly alters the slope of the curve beyond the equilibrium distance, changing it from negative for the 26*s*20*p*14*d*2*f* basis to positive for the large 28*s*22*p*17*d*5*f*3*g*2*h* basis. A similar qualitative picture holds for the NR-CCSD(T) method. From these observations we conclude that the negative slopes obtained by Maroulis and by Ilias *et al*. reflect a cancellation of errors—the use of too small a basis set and the lack of SOC.

The close agreement between the experimental radial function of the electric dipole moment of HI and the DC-CCSD(T) function enables us to conclude that previously expressed doubts about the accuracy of the experimental dipole moment on the basis of theoretical work are not well founded. The gap between calculation and experiment becomes closed through the use of a large basis set, including the *g* and *h* functions, and the inclusion of SOC.

Spectral parameters

The agreement between the DC-CCSD(T) values and experiment for the spectral parameters, according to Table 4, is satisfactory overall. The SFDC-CCSD(T) method also agrees satisfactorily with experiment, except for D_e because it lacks the spin–orbit splitting of the H(^1S)+I(^2P) asymptote. For all calculated spectral parameters, the SFDC-CCSD(T) values that are corrected with HF SOC contributions result in almost the same values as the full DC-CCSD(T) values, at a much smaller computational cost because single-group symmetry suffices for SFDC-CCSD(T) calculations. Visscher *et al.*[43] calculated the effect of inclusion of the two-electron Gaunt interaction on R_e, ω_e and D_e of HI; the effect found on R_e was an increase of 0.1 pm, on ω_e a decrease of 2 cm^{-1}, and a negligible effect on D_e. Also, shown in Table 4 are the results from Feller *et al.*,[44] who used a newly designed large aug-cc-pRV5Z basis set for use with a small-core RECP. For D_e their result agrees better with experiment than our DC-CCSD(T) value, with deviations 3.4 and 4.6 kJ mol^{-1}, respectively. For the calculation of D_e, Feller *et al*. applied, besides the use of a RECP, scalar relativistic corrections and SOC corrections that are expected to approach the Dirac–Coulomb–Breit limit. Rather than the difference in Hamiltonians, the reason for their superior agreement with experiment is likely to be the still greater quality of their basis set. For R_e and ω_e, their agreement with experiment is worse than ours; two reasons for this condition might be that for these properties they applied no extra relativistic correction, beyond the use of a RECP, and that their FCI estimation was based on a continued-fraction approximation,[45] which might in some cases improve the results but worsen them in others.

V Conclusion

The satisfactory agreement between quantum-chemical computations and experimentally observable molecular properties of HI, specifically the frequencies and intensities of vibration-rotational transitions, indicates both a mature state of calculations of molecular electronic structure involving atoms of fairly large atomic number and the efficacy of the Dunham approach to analysis of vibration-rotational spectra. Our work provides no support for doubt about the accuracy of the experimental dipole moment because the discrepancy between theory and experiment becomes resolved through the use of a large basis set, including *g* and *h* functions, and the inclusion of spin–orbit coupling in a variational manner. Our predictions of matrix elements for intensities of vibrational transitions for the fifth and sixth overtone bands of HI can serve as guides for experimental measurements of these properties.

Acknowledgements

JNPvS and LV thank the Netherlands Organisation for Scientific Research (NWO) for financial support through the 'Jonge Chemici' program, the Dutch National Computing Facilities (NCF) for computer time, and EU COST action D26, WG HAMEC for travel support. JFO thanks Dr. J.-P. Bouanich for helpful discussion.

References

1 M. Ilias, V. Kellö, T. Fleig and M. Urban, *Theor. Chem. Acc.*, 2003, **110**, 176–184.
2 J. F. Ogilvie, *The Vibrational and Rotational Spectrometry of Diatomic Molecules*, Academic Press, London, 1998.
3 S. R. Ungemach, H. F. Schaefer III and B. Liu, *J. Mol. Spectrosc.*, 1977, **66**, 99–105.
4 H.-J. Werner, E. A. Reinsch and P. Rosmus, *Chem. Phys. Lett.*, 1981, **78**, 311–315.
5 P. Schwerdtfeger, L. V. Szentpály, K. Vogel, H. Silberbach, H. Stoll and H. Preus, *J. Chem. Phys.*, 1986, **84**, 1606–1612.
6 D. A. Chapman, K. Balasubramanian and S. H. Lin, *J. Chem. Phys.*, 1987, **87**, 5325–5328.
7 D. A. Chapman, K. Balasubramanian and S. H. Lin, *Phys. Rev. A*, 1988, **38**, 6098–6106.
8 V. Kellö and A. J. Sadlej, *J. Chem. Phys.*, 1990, **93**, 8122–8132.
9 M. Dolg, *Mol. Phys.*, 1996, **88**, 1645–1655.

10 E. van Lenthe, J. G. Snijders and E. J. Baerends, *J. Chem. Phys.*, 1996, **105**, 6506–6516.
11 G. Maroulis, *Chem. Phys. Lett.*, 2000, **318**, 181–189.
12 A. B. Alekseyev, H.-P. Liebermann, D. B. Kokh and R. J. Buenker, *J. Chem. Phys.*, 2000, **113**, 6174–6185.
13 P. Norman, B. Schimmelpfennig, K. Ruud, H. J. Aa. Jensen and H. Ågren, *J. Chem. Phys.*, 2002, **116**, 6914–6923.
14 O. Fossgaard, O. Gropen, M. C. Valero and T. Saue, *J. Chem. Phys.*, 2003, **118**, 10418–10430.
15 F. A. van Dijk and A. Dymanus, *Chem. Phys. Lett.*, 1970, **5** 387–389.
16 G. Ameer and W. M. Benesch, *J. Chem. Phys.*, 1962, **37** 2699–2702.
17 P. Niay, P. Bernage, C. Coquant and A. Fayt, *J. Mol. Spectrosc.*, 1978, **72**, 168–171.
18 H. Riris, C. B. Carlisle, D. E. Cooper, L.-G. Wang, T. F. Gallagher and R. H. Tipping, *J. Mol. Spectrosc.*, 1991, **146** 381–388.
19 M. O. Bulanin, A. V. Domanskaya and K. Kerl, *J. Mol. Spectrosc.*, 2003, **218**, 75–79.
20 W. M. Benesch, *J. Chem. Phys.*, 1963, **39**, 1048–1052.
21 P. C. Meyer, C. Haeusler and P. Barchewitz, *J. Phys.*, 1965, **26**, 305–316.
22 M. O. Bulanin, A. V. Domanskaya, I. M. Grigoriev and K. Kerl, *J. Mol. Spectrosc.*, 2004, **223**, 67–72.
23 P. Niay, P. Bernage, C. Coquant and R. Houdart, *Can. J. Phys.*, 1978, **56**, 727–736.
24 C. Haeusler, *Ph.D. Thesis*, University of Paris, Paris, 1965.
25 J. A. Pople, *Rev. Mod. Phys.*, 1999, **71**, 1267–1274.
26 P. Pyykkö, *Chem. Rev.*, 1988, **88**, 563–594.
27 L. Visscher, T. Enevoldsen, T. Saue and J. Oddershede, *J. Chem. Phys.*, 1998, **109**, 9677–9684.
28 J. N. P. van Stralen and L. Visscher, *Mol. Phys.*, 2003, **101** 2115–2124.
29 A. J. Sadlej, *Collect. Czech. Chem. Commun.*, 1988, **53**, 1995–2016.
30 J. N. P. van Stralen and L. Visscher, *J. Chem. Phys.*, 2002, **117**, 3103–3108.
31 T. Helgaker, P. Jørgensen and J. Olsen, *Molecular Electronic Structure Theory*, Wiley, Chichester, 2000.
32 J. M. Lévy-Leblond, *Commun. Math. Phys.*, 1967, **6**, 286.
33 K. G. Dyall, *J. Chem. Phys.*, 1994, **100**, 2118–2127.
34 T. Saue, V. Bakken, T. Enevoldsen, T. Helgaker, H. J. Aa. Jensen, J. K. Laerdahl, K. Ruud, J. Thyssen and L. Visscher, *Dirac, a relativistic ab initio electronic structure program, Release 3.2*, 2000.
35 L. Visscher, *Theor. Chem. Acc.*, 1997, **98**, 68.
36 R. J. Le Roy, *LEVEL 7.4: A computer program for solving the radial Schrödinger equation for bound and quasibound levels*, University of Waterloo Chemical Physics Research, Report No. CP-642-R, 2001.
37 M. W. Chase, *J. Phys. Chem. Ref. Data Monogr.*, 1998, **9**.
38 C. A. Burris, *J. Chem. Phys.*, 1959, **30**, 976.
39 J. F. Ogilvie, J. Oddershede and S. P. A. Sauer, *Adv. Chem. Phys.*, 2000, **111**, 475–536.
40 J. F. Ogilvie, W. R. Rodwell and R. H. Tipping, *J. Chem. Phys.*, 1980, **73**, 5221–5229.
41 F. M. Fernandez and J. F. Ogilvie, *MapleTech*, 1998, **5**, 42–46.
42 X. Li and J. Paldus, *J. Chem. Phys.*, 1998, **108**, 637–648.
43 L. Visscher, J. Styszynski and W. A. Nieuwpoort, *J. Chem. Phys.*, 1996, **105**, 1987–1994.
44 D. Feller, K. A. Peterson, W. A. de Jong and D. A. Dixon, *J. Chem. Phys.*, 2003, **118**, 3510–3522.
45 D. Z. Goodson, *J. Chem. Phys.*, 2002, **116**, 6948.
46 F. C. de Lucia, P. Helminger and W. Gordy, *Phys. Rev. A*, 1971, **3**, 1849–1857.
47 B. Rosenblum and A. H. Nethercot, *Phys. Rev.*, 1955, **97**, 84–85.
48 K. V. Chance, T. D. Varberg, K. Park and L. R. Zink, *J. Mol. Spectrosc.*, 1993, **162**, 120–126.
49 T. D. Varberg, J. C. Roberts, K. A. Tuominen and K. M. Evenson, *J. Mol. Spectrosc.*, 1998, **191**, 384–386.
50 A. Goldman, K. V. Chance, M. T. Coffey, J. W. Hannigan, W. G. Mankin and C. P. Rinsland, *J. Quant. Spectrosc., Radiat. Transfer*, 1998, **60**, 665–710.
51 P. Guelachvili, P. Niay and P. Bernage, *J. Mol. Spectrosc.*, 1981, **85**, 253–270.
52 P. Niay, P. Bernage, H. Bocquet and R. Houdart, *J. Mol. Spectrosc.*, 1979, **77**, 133–138.
53 T. Katayama, F. Matsushima and H. Sasada, *J. Mol. Spectrosc.*, 1994, **167**, 236–237.